© 2002 The Chemical Society of Japan *Bull. Chem. Soc. Jpn.*, **75**, 2289–2296 (2002) 2289

Sonolytic Control of Rate of Gold(Ⅲ) Reduction and Size of Formed Gold Nanoparticles: Relation between Reduction Rates and Sizes of Formed Nanoparticles

Kenji Okitsu,* Akihiko Yue,† Shuji Tanabe,† Hiroshige Matsumoto,† Yoshihiro Yobiko,†† and Youngeok Yoo†††

Japan Science and Technology Corporation, 4-1-8 Hon-cho, Kawaguchi, Saitama 332-0012

†Faculty of Engineering, Nagasaki University, 1-14 Bunkyo-machi, Nagasaki 852-8521

††Technology Research Institute of Osaka Prefecture, 2-7-1 Ayumino, Izumi, Osaka 594-1157

†††Department of Environmental Education, Daegu University, 15 Naeri, Jinryang, Kyungsan, Kyungbuk 712-714, Korea

(Received April 22, 2002)

The sonochemical reduction of gold(Ⅲ) [tetrachloroaurate(Ⅲ)] was carried out under various irradiation conditions in an aqueous solution containing only a small amount of 1-propanol. Identical starting materials and the same initial concentrations were used in each preparation. The rates of gold(Ⅲ) reduction were strongly dependent on the atmosphere, the temperature of the bulk solution, the intensity of the ultrasound, and the distance of the reaction vessel from the oscillator. For example, the rates of reduction under several atmospheres were in the order of $CH_4 = CO_2 < N_2 <$ Ne $<$ He $<$ Ar $<$ Kr, where no reduction proceeded under the CH_4 and CO_2 atmospheres. It was clearly found that the rates of reduction were influenced by the cavitation phenomenon. Upon irradiation, colloidal gold particles having a surface plasmon absorption were formed, although in the absence of any stabilizers for the gold particles. It was found by TEM observations that the average size of the formed gold particles changed from 30 to 120 nm by selecting the irradiation parameters. The size of the gold particles was closely correlated to the initial rate of gold(Ⅲ) reduction; the higher the rate of reduction, the smaller the particles. This relationship suggested that the rate of reduction would affect the initial gold nucleation processes. In a 200 kHz standing wave system used in the present study, the strength of the generated shock waves as well as the mechanical effects could be regarded as relatively weak.

Gold nanoparticles have been widely applied to various materials, such as analytical probes,[1] biological markers,[2] colorings,[3] catalysts,[4] sensors,[5] and nonlinear optics materials.[6] Such versatile applications are mainly based on the interesting physicochemical properties arising from the size effects of the gold nanoparticles. In fact, due to the growing need to develop a simple method for preparing such functional metal nanoparticles, a number of techniques have been reported during the last decade. Most of the studies in colloid science are focused on the control of the size, shape, and structure of metal nanoparticles from a practical point of view.[7] In addition, a controlled-chemical reduction system in an appropriate solution is suggested to be one of the most promising methods in recent years.[7] The mechanism of formation of noble metal nanoparticles including gold, however, has not yet been clarified, particularly in a solution system using the reduction process of noble metal ions. The reasons that the mechanism could not be clarified in detail are presumably attributed to the following reasons: There have been difficulties in (Ⅰ) the quantitative analysis of the concentration of unreduced metal ions coexisting with the formed colloidal particles and their stabilizer in a solution, (Ⅱ) the precise determination of the rate of reduction of metal ions because the rate was often too fast to trace the course of the reduction, and (Ⅲ) the control of the rate of reduction in conventional thermal reduction systems. Especially, it is very difficult to control the rate of reduction using identical starting materials and the same initial concentrations. Thus far, most of the studies for producing size-controlled particles have been based on the change in the amounts, types and combinations of the starting materials such as metal ions, reducing agents and stabilizers.[7] Based on these reasons, there are very few reports that provide a clear relationship between the rate of reduction of noble metal ions and the size of the formed metal particles in the solution systems. If both the mechanisms of the reduction of metal ions and of the formation of the colloidal metal could be clarified in more detail, advances in the field of colloid science as well as advances in nano-technology should be achieved.

This manuscript describes the sonochemical formation of gold nanoparticles without any stabilizers and the rates of gold(Ⅲ) reduction are quantitatively estimated under various irradiation conditions using a colorimetric method. Locally generated multi-bubbles with an extremely high temperature and high pressure are used for the sonochemical reactions. Nagata et al. and one of the authors[8] previously reported the effect of various organic additives on the rate of gold(Ⅲ) reduction under ultrasonic irradiation. Here it was clearly indicated that organic additives with the appropriate hydrophobic property enhanced the rates of reduction. For example, alcohols, ketones, surfactants and water-soluble polymers acted as accelerators for the reduction of noble metals ions under ultrasonic irradiation.[8,9] Grieser and co-workers[10] also reported the effect of alcohol additives on the reduction of gold(III). They insisted that the rate of the sonochemical reduction of gold(III) was related to the Gibbes surface excess concentration of the alcohol additives. The average sizes of the sonochemically formed gold particles were less than 10 nm in the presence of dodecyl sodium sulfate.[8] Although ultrasonic cavitation has been used in the preparation of various types of transition metal nanoparticles during the last decade,[11] to our knowledge, there are only a few reports related to the rate-control of metal formation and the size-control of the formed particles. In a previous communication, we have preliminary reported that the size of the formed gold particles changed by selecting the parameters involving the irradiation conditions and procedures.[12] In this study, we performed a further detailed investigation on various parameters influencing the rates of the gold(III) reduction and the size of the formed gold particles, in which identical starting materials were used in each preparation to clarify the net effect of the rate of gold(III) reduction on the size of the formed gold particles. The effects of ultrasonic cavitation on the rate of reduction and on the behavior of the formed colloidal particles are also discussed.

Experimental

Reagents. Reagent-grade $Na[AuCl_4]\cdot 2H_2O$, 1-propanol, $FeSO_4\cdot 7H_2O$, H_2SO_4, NaBr, and α-Al_2O_3 (a nominal particle size of 0.5 µm) were purchased from Wako and used without further purification. All the water used in the present experiment was treated by a conventional ion-exchange and distillation procedure. Helium, neon, argon, krypton, nitrogen, carbon dioxide and methane of more than 99.99% purity were obtained from Japan Air Liquid, Nippon Sanso and Sumitomo Seika.

Procedure of Ultrasonic Irradiation. Ultrasonic irradiation was carried out using an ultrasonic generator (Kaijo 4021type; Lot. No. Y232, frequency; 200kHz) and a 65 mm ϕ barium titanate oscillator (Kaijo; Lot. No. Y300), which was operated at ca. 20 to 200 W in a water bath maintained at a constant temperature. The irradiation set-up and the characteristics of the reaction vessel used are illustrated in Fig. 1. The glass vessel was cylindrical and it had a port covered by a silicon rubber septum for gas bubbling or sampling without exposing the sample to air. The bottom of the vessel was planar, 1 mm thick and 55 mm ϕ in diameter. An aqueous solution of $Na[AuCl_4]$ (1.0 mM, 65 mL) was added to the vessel and then it was purged with the appropriate gas. As an accelerator for the gold(III) reduction, 1-propanol was injected into the gas-purged solution, corresponding to a 20 mM concentration. In order to minimize the effects of the 1-propanol molecules on the nucleation or growth of the gold particles, a very small amount of 1-propanol was added in the present study. Various irradiation parameters were selected, such as the atmosphere, the temperature of the solution, the intensity of the ultrasound, and the distance between the reaction vessel and the oscillator. During the course of the irradiation, the vessel was closed from the air atmosphere. On the other hand, the ultrasonic power injected into the sample solution was measured by a calorimetric method, as described elsewhere.[13] In addition, the rate of H_2O_2 formation in the sonolysis of Ar-saturated water was estimated by a method similar to Fricke dosimetry:[8] A 65 mL of Ar-saturated aqueous solution containing 50 mM $FeSO_4$ and 0.8 N H_2SO_4 was irradiated and then the amount of Fe(III) ions ($\varepsilon = 2194$ M^{-1} cm^{-1}, $\lambda = 304$ nm) formed from H_2O_2 and $^{\bullet}OH$ oxidation of Fe(II) was spectrophotometrically measured.

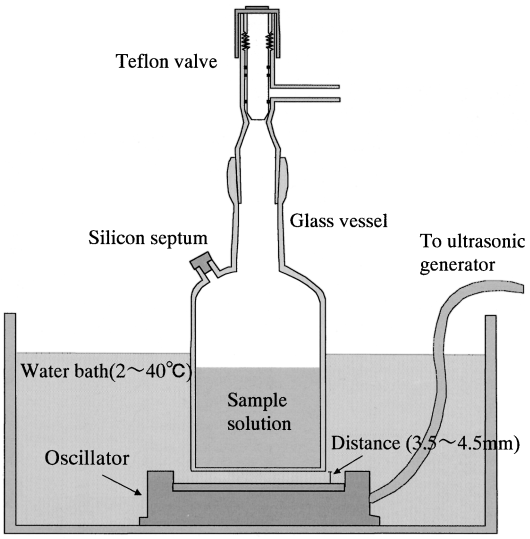

Fig. 1. Standing-wave type irradiation system.

Colorimetric Analysis. The absorption spectra of the irradiated solutions were measured by an UV-vis spectrophotometer (Shimadzu UV-2100). The concentration of gold(III) in the irradiated solution was determined by a colorimetric method using NaBr,[8,14] i.e., the absorption peak of $[AuBr_4]^-$, which was formed in a ligand exchange reaction between Cl^- and Br^-, was clearly observed at 382 nm by the addition of saturated NaBr solution to the sample solution containing the unreduced $[AuCl_4]^-$. At the same time, the aggregation of the colloidal gold particles rapidly occurred. The colorimetric analysis was, therefore, carried out for the solution filtered through a membrane filter with a pore-size of 0.2 µm to avoid any spectrophotometric interference of the gold aggregates formed after the addition of the NaBr solution.

Characterization of the Formed Gold Nanoparticles. The sonochemically formed gold particles were observed using a transmission electron microscope (TEM, JEOL JEM-100S) at an acceleration voltage of 100 kV. Specimens for the TEM observations were prepared as follows: The irradiated solution (irradiation time, 20 min) was immediately mixed with an aqueous suspension of alumina powders to immobilize the formed gold particles on the surface of the alumina. This procedure was carried out to avoid aggregation of the formed gold particles during the subsequent drying processes. The sonochemically formed gold particles were rapidly immobilized on the surface of the alumina powders so that the color of the solution became transparent. On the other hand, the white alumina powders were tinged reddish purple. The suspension composed of the gold particles immobilized on the alumina powders was filtered and washed with distilled water. The aqueous suspension of such powders was then dropped onto a Cu grid coated with a collodion film and then dried in a vacuum.

Results and Discussion

Sonochemical Reduction of Gold(III). The reduction of gold(III) smoothly proceeded upon irradiation, which could be attributed to the formation of reducing species from the 1-propanol and water sonolysis. The chemical reactions induced by the ultrasonic irradiation of a liquid are known to result from a cavitation phenomenon and the sites of the sonochemical reactions are characterized by three different regions in an aqueous solution system: (1) The inside of the collapsing cavitation bubbles where several thousands of degrees and more than hundreds of atmospheres are produced.[15,16] (2) The interfacial region between the cavitation bubbles and the bulk solution where the temperature is lower than the inside of the cavitation bubbles but still high enough for thermal decomposition of the solutes to occur. (3) The bulk solution at ambient temperature where the reactions of the solute molecules with various radicals and unstable species, which escaped from the interfacial region, take place.

According to many previous reports about sonochemistry, it is predictable that the chemical reactions induced by the ultrasonic cavitation should be sensitively influenced by the irradiation conditions and procedures. In this study, various ultrasonic parameters influencing the rates of the gold(III) reduction were investigated. The dependence of the ultrasonic intensities on the rates of reduction were first considered. Figure 2 shows the changes in the concentration of gold(III) for several ultrasound intensities, in which the intensities were evaluated by the calorimetric method. It was clearly observed that the concentration of gold(III) rapidly decreased with the irradiation time and the reduction completely was finished within the 20min irradiation of 1.20 and 1.43 W cm^{-2}. The rates of gold(III) reduction changed by the ultrasound intensities. The initial rates of the gold(III) reduction are summarized in Fig. 3. To discuss the relation between the rates of reduction and the cavitation phenomenon, the rates of H_2O_2 formation are also plotted in Fig. 3, in which the rates of H_2O_2 formation are measured from the water sonolysis in the absence of gold(III) and 1-propanol. Both the rates of gold(III) reduction and of H_2O_2 formation were also found to increase with the increasing intensities. In addition, the threshold value of the gold(III) reduction seemed to be smaller than that of the H_2O_2 formation.

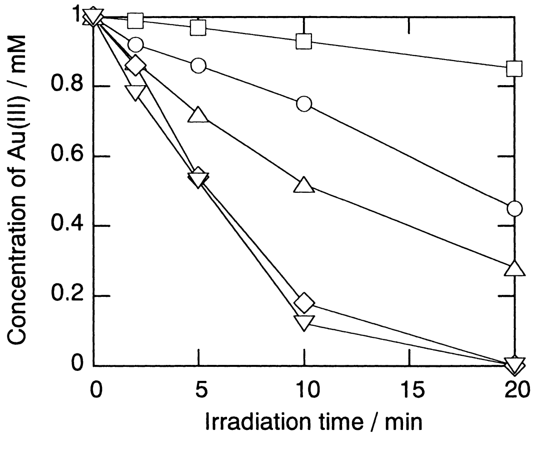

Fig. 2. Changes in the concentration of Au(III) during ultrasonic irradiation under various intensities. Condition: 1-propanol; 20 mM, Ar atmosphere, temperature; 20 °C, distance; 4.0 mm. (□) 0.15 W cm^{-2}, (○) 0.53 W cm^{-2}, (△) 0.92 W cm^{-2}, (◇) 1.20 W cm^{-2}, (▽) 1.43 W cm^{-2}.

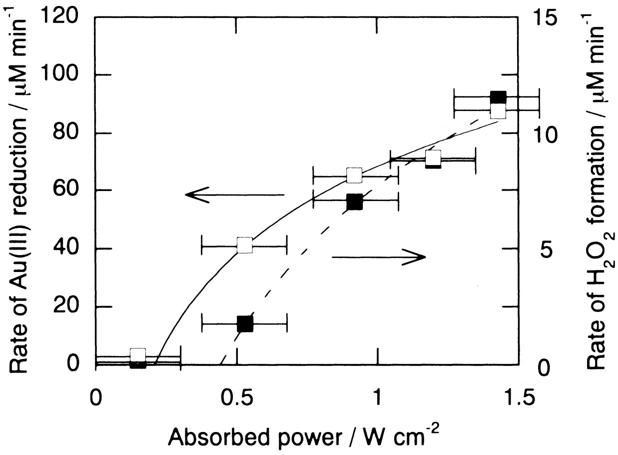

Fig. 3. Rate of Au(III) reduction (□) in the presence of 20 mM 1-propanol and rate of H_2O_2 formation (■) in pure water under various intensities. Condition: Ar atmosphere, temperature; 20 °C, distance; 4.0 mm.

Nagata et al. and one of the authors previously reported that the sonochemical reduction of gold(III) readily occurred in an aqueous solution due to the addition of organic compounds, such as alcohols, ketones, surfactants and water-soluble polymers.[8] It was found that organic additives are a source of reducing species under sonication and that the rate of gold(III) reduction strongly depended on the types and amounts of such organic additives. The reduction pathways via several reducing species have also been suggested in the presence of an alcohol, RHOH, as follows. Equations 1–4 show the common basal reactions in aqueous sonochemistry,

$$H_2O \xrightarrow{)))} {}^{\bullet}OH + {}^{\bullet}H \tag{1}$$

$$2{}^{\bullet}OH \rightarrow H_2O_2 \tag{2}$$

$$2{}^{\bullet}H \rightarrow H_2 \tag{3}$$

$${}^{\bullet}OH + {}^{\bullet}H \rightarrow H_2O \tag{4}$$

where the symbol of))) indicates the action of ultrasonic irradiation. The reducing species of H atoms and H_2 molecules are formed during the sonolysis of water. The rates of gold(III) reduction by H atoms and H_2 molecules, however, might be actually slow, although the rate constants in both cases are extremely high.[8,17] The RHOH molecules that accumulated on the interface of the cavitation bubbles also rapidly react with active radicals as follows:

$$RHOH + {}^{\bullet}OH({}^{\bullet}H) \rightarrow {}^{\bullet}ROH + H_2O(H_2) \tag{5}$$

where secondary reducing radicals, ${}^{\bullet}$ROH, are formed by hydrogen abstraction from RHOH with OH radicals and H atoms. Strong oxidants such as OH radicals are advantageously quenched and H_2 molecules are also generated in this reaction. Furthermore, the RHOH molecules are pyrolyzed at the interface and the inside of the bubbles,[18]

$$\mathrm{RHOH} \rightarrow \text{Pyrolysis products} \tag{6}$$

where a part of the pyrolysis products also correspond to reducing species.[8] Several types of reducing species subsequently react with gold(III) to form gold metal particles.

$$\mathrm{Au^{3+} + H_2O + RHOH} \overset{)))}{\rightarrow\rightarrow\rightarrow} \mathrm{Au^0 + 3H^+} + \text{products} \tag{7}$$

$$n\mathrm{Au^0} \rightarrow (\mathrm{Au^0})_n \tag{8}$$

Gold(II) ions might be formed in the reduction processes, but they are very unstable so that the following disproportionation reaction would also occur.[19]

$$2\mathrm{Au^{2+}} \rightarrow \mathrm{Au^+ + Au^{3+}} \tag{9}$$

As seen in Fig. 3, it was found that the rates of gold(III) reduction were ca. 8–24 times faster than those of the H_2O_2 formation for each ultrasound intensity. In particular, the rate of H_2O_2 formation was extremely slow when the intensity of the ultrasound was weak, while the rate of gold(III) reduction seemed to be relatively fast. This result implies that the reduction pathways, as mentioned above, might be different among the different ultrasound intensities. The results in Fig. 3 roughly suggest that the reduction of gold(III) proceeds via pyrolysis radical species (formed by Eq. 6) as the main reduction pathway and the reduction via secondary reducing radicals (formed by Eq. 5) could be regarded as a minor reaction pathway, particularly at low intensity around the threshold value of the water sonolysis. Riesz and co-workers previously reported that various pyrolysis radicals were formed in the sonolysis of alcohol-aqueous solutions, which were determined by a spin trapping ESR method.[18] It is reasonable that pyrolysis radicals are also formed in the present irradiation system because the pyrolysis of water molecules easily occurs. As seen in Figure 3, the difference in the threshold values between the gold(III) reduction and the H_2O_2 formation might be attributed to the ease of pyrolysis between the 1-propanol and water molecules. On the other hand, it was also recognized that no reduction occurred using a conventional ultrasonic cleaner (Honda Electric Co., W-113, 28kHz, 100W, Bath-volume: ca. 2 L). These results mean that the gold(III) reduction requires sufficiently hot bubbles which cause pyrolysis of the water and 1-propanol molecules. The temperatures and/or number of cavitation bubbles should increase with the increasing intensity in the present irradiation system.

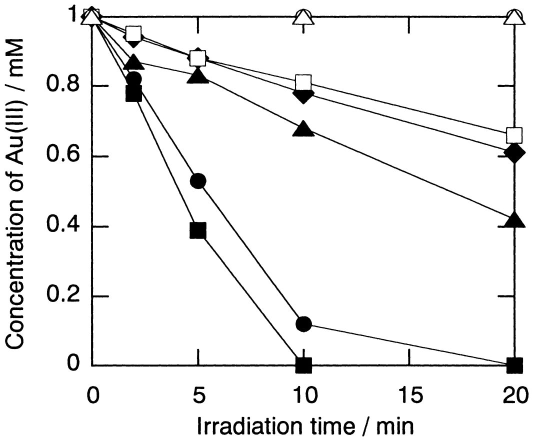

Fig. 4. Changes in the concentration of Au(III) during ultrasonic irradiation under various atmospheres. Condition: Intensity; 1.43 W cm^{-2}, 1-propanol; 20 mM, temperature; 20 °C, distance; 4.0 mm. (■) Kr, (●) Ar, (▲) Ne, (◆) He, (□) N_2, (○) CO_2, (△) CH_4.

Figure 4 shows the effect of the atmospheric gases on the sonochemical reduction of gold(III). It was observed that the rates of reduction were strongly dependent on the irradiated atmospheres in spite of the ultrasound intensity being the same in all cases. In general, the cavitation effects are well-known to be influenced by the physical properties of the atmospheric gases such as the ratio of specific heats, $\gamma = C_p/C_v$, the thermal conductivity, and the solubility. The γ value is one of the most important factors influencing the attained temperature inside the collapsing bubbles, according to the hot spots theory.[20] The maximum temperature in the collapsing bubble, T_{max}, could be roughly determined by the following equation:

$$T_{max} = T_0 P_{max}(\gamma - 1)/P \tag{10}$$

where T_0 is the temperature of the sample solution, P_{max} is the maximal pressure in the liquid at the moment of transient collapse, and P is the sum of the vapor pressure of the solvent and the atmospheric gas pressure. As seen in Fig. 4, the rates of reduction under the noble gas atmospheres were faster than those under the polyatomic molecule gas atmospheres. Under the CO_2 and CH_4 atmospheres, no reduction proceeded at all. This result was in good agreement with the order of the γ values, which increase in the order of CH_4 (γ;1.3) = CO_2 (1.3) < N_2 (1.4) < noble gases (ca. 1.6–1.7). Furthermore, different rates were also observed among the noble gas atmospheres. The rates were in the order of He < Ne < Ar < Kr. This order was consistent with the attained temperature inside the collapsing bubbles as previously reported.[21] The maximum temperature inside the collapsing bubbles would decrease with the increasing thermal conductivity of the gases, where the conductivity (10^{-4} W m^{-1} K^{-1}) was in the order of He (1499) > Ne (493) > Ar (177.2) > Kr (94.2) at 1atm and 300 K.[22] Furthermore, it has also been suggested that the solubility of the gases might contribute to the number of cavitation bubbles:[16] the solubility in water (cm^3 kg^{-1}) increases in the order of He (9.375) < Ne (11.15) < Ar (36.60) < Kr (66.98) at 1atm and 293.15 K.[23] By using such atmospheric parameters, the rates of the sonochemical reduction of gold(III), as well as of noble metal ions, should be controlled.

Figures 5 and 6 show the initial rates of gold(III) reduction obtained under additional irradiation parameters. Figure 5 indicates the effects of the distance from the oscillator to the bottom of the reaction vessel. The maximum rate of reduction

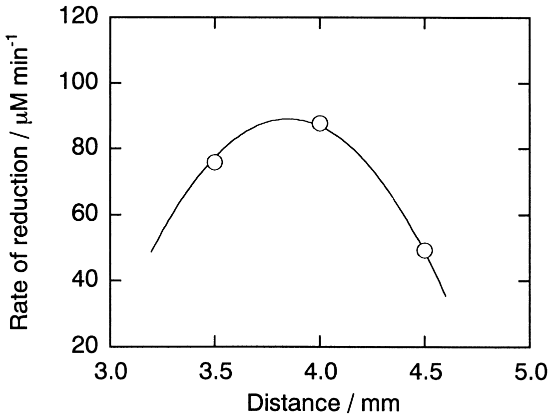

Fig. 5. Rate of Au(III) reduction as a function of the distance between the reaction vessel and the oscillater. Condition: Intensity; 1.43 W cm^{-2}, Ar atmosphere, temperature; 20 °C.

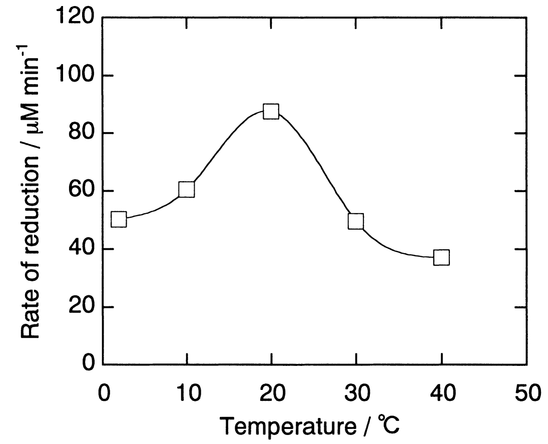

Fig. 6. Rate of Au(III) reduction as a function of the temperature of the bulk solution. Condition: Intensity; 1.43 W cm^{-2}, Ar atmosphere, distance; 4.0 mm.

was seen at the distance of ca. 3.8 mm, which was approximately consistent with the half-wavelength of the ultrasound (3.71 mm) used in the present study. This result could be explained as follows: The sound is effectively transmitted into the reaction vessel when the node plane formed in the standing wave system is located just at the bottom of the vessel.[24]

Figure 6 shows the influence of the bulk solution temperature. It was recognized that the initial rates of reduction sensitively changed in spite of a small change in the temperature from 2 to 40 °C. The rate increased by increasing the temperature up to 20 °C, but it decreased at higher temperatures. This result could be elucidated by the following cavitation phenomenon: In the range of 2 to 20 °C, as the temperature of the bulk solution increases, the water and alcohol molecules are more easily vaporized in the cavitation bubbles, resulting in the effective formation of reducing species which promote the reduction. On the other hand, when the temperature of the solution further increased, the temperature generated in the collapsing bubble does not elevate due to the cushion effect which was caused by the incorporation of an excess amount of water and alcohol molecules into the bubble. The cushion effect could be theoretically explained on the basis of Eq. 10, as follows: When the temperature of the bulk solution (T_0) increases, T_{max} becomes lower because the value of P steeply increases with the increasing amount of water and 1-propanol vapor inside the bubble. In addition, the value of γ also decreases because the γ value of water and 1-propanol is substantially lower than that of argon gas (e.g., $\gamma = 1.67$ for argon, ca. 1.3 for water and ca. 1.1 for 1-propanol). Consequently, the maximum temperature in the cavitation bubbles drops with increasing the amount of water and 1-propanol vapor inside the bubble. Thus, the amounts of reducing species decrease for a higher temperature solution. This speculation was also supported by other reports[25,26] in which the relation between the solvent and/or solute vapor in the collapsing bubbles and its decomposition efficiency was clearly indicated.

Formation of Gold Nanoparticles. The color of the solution rapidly changed from an initial pale yellow to reddish purple due to the ultrasonic irradiation. UV-vis spectral analyses indicated that a surface plasmon absorption attributed to the colloidal gold particles had emerged. This result suggests the progress of the gold(III) reduction and the formation of gold nanoparticles, as seen in Eqs. 7 and 8. The sonochemically formed gold metals were characterized by TEM spectroscopy. To avoid aggregation of the formed gold particles during the preparation of the TEM specimens, we added submicron-sized alumina powders immediately after the sonochemical reduction.

Figure 7 shows representative TEM photographs in which the ultrasonic intensity is the only changing irradiation parameter. A number of small gold particles immobilized on the alumina surface were clearly observed and the formation of spherical gold particles was recognized in each preparation. For example, the average size of the gold particles was 53.8 nm at 0.92 W cm^{-2}, 50.8 nm at 1.20 W cm^{-2}, and 35.5 nm at 1.43 W cm^{-2}, respectively. Since no stabilizer was used in the present preparation, the particle sizes were slightly larger compared to those prepared in the presence of suitable stabilizers.[8]

The gold particles prepared by the other irradiation parameters were also characterized. Table 1 shows the initial rates of the gold(III) reduction, the average size of the formed gold particles and the reduction ratio under various irradiation conditions. The standard deviation (SD) of the size of the formed gold particles is also indicated in Table 1. The sizes of the formed gold particles were found to sensitively change with the irradiation parameters. To clarify the relation between the rate of gold(III) reduction and the size of the formed gold particles, we plotted the experimental data in Fig. 8. Despite the different irradiation conditions, it was clearly recognized that the size of the gold particles decreased with an increase in the rate of gold(III) reduction. If shock waves generated by ultrasonic irradiation affected the growth of the gold particles, the size of the particles might become larger with stronger shock waves. According to the results of Fig. 3, one can notice that the rate of gold(III) reduction is closely related to the absorbed ultrasonic power, which should correspond to the strength of the cavitation. Therefore, the strength of shock waves must become greater when the rate of gold(III) reduction is higher, assuming a simple dependence of the cavitation strength vs the absorbed ultrasonic power. To allow us to consider the effect of the ultrasonic intensities on the particle sizes, the sizes

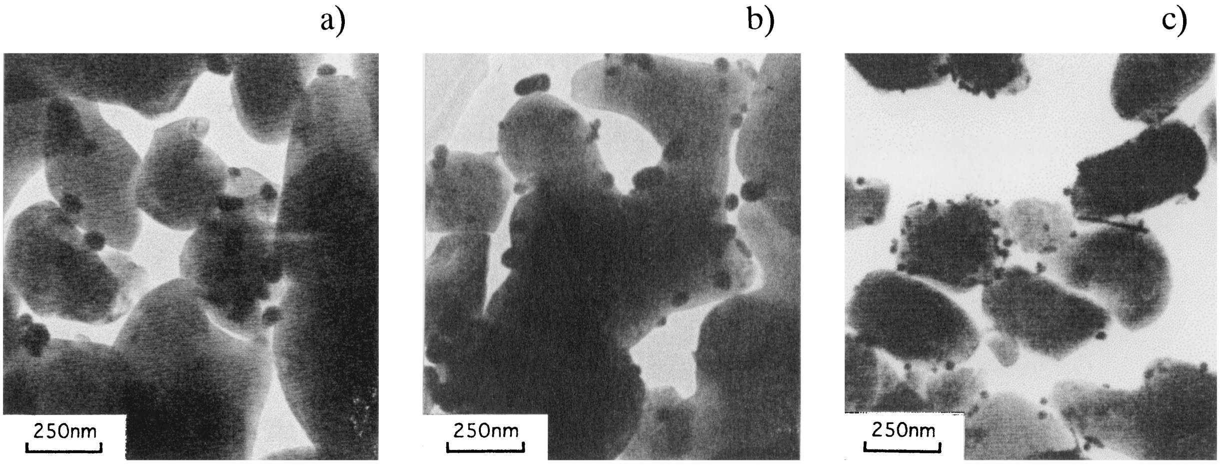

Fig. 7. Effect of the ultrasonic intensity on the size of the formed Au nanoparticles. Condition: 1-propanol; 20 mM, Ar atmosphere, temperature; 20 °C, distance; 4.0 mm, irradiation time; 20 min. (a) 0.92 W $\mathrm{cm^{-2}}$, (b) 1.20 W $\mathrm{cm^{-2}}$, (c) 1.43 W $\mathrm{cm^{-2}}$.

Table 1. Initial Rate of Au(III) Reduction, Average Size of Sonochemically Formed Au Particles and Reduction Ratio under Various Irradiation Conditions

Run	Parameters			Initial rate of reduction /μM $\mathrm{min^{-1}}$	Average size ± SD/nm	Reduction ratio[b]/%
	Intensity of ultrasound /W $\mathrm{cm^{-2}}$	Temperature of bulk solution/°C	Distance[a] /mm			
1	0.53	20	4.0	41.1	125.7 ± 52.7[c]	55
2	0.92	20	4.0	65.1	53.8 ± 16.6	78
3	1.20	20	4.0	71.3	50.8 ± 17.1	100
4	1.43	20	4.0	87.5	35.5 ± 8.0	100
5	1.43	20	3.5	75.8	33.3 ± 8.5	98
6	1.43	20	4.5	49.2	71.8 ± 16.4	84
7	1.43	40	4.0	37.0	71.5 ± 19.0	63
8	1.43	30	4.0	49.5	58.3 ± 16.1	74
9	1.43	2	4.0	50.2	40.3 ± 11.4	79
10	1.43	10	4.0	60.4	41.6 ± 10.1	100

a) Distance between reaction vessel and oscillator, b) Reduction ratio at 20 min irradiation. c) The number of measurments are not enough.

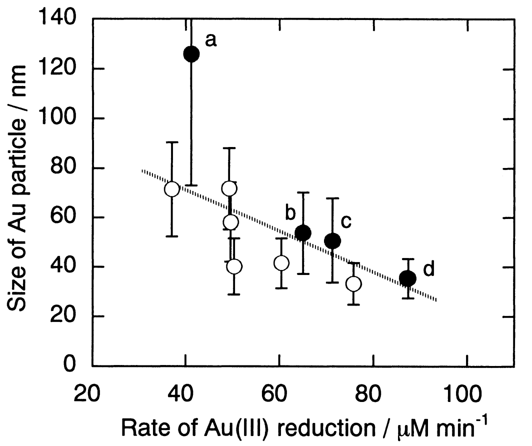

Fig. 8. Relation between the rate of Au(III) reduction and the average size of the formed gold particles. Each error bar corresponds to the standard deviation of the size of the gold paritcles. Closed circles correspond to the dependence of the ultrasonic intensities, in which the rate of reduction increases with increasing the intensity. (a) 0.53 W $\mathrm{cm^{-2}}$, (b) 0.92 W $\mathrm{cm^{-2}}$, (c) 1.20 W $\mathrm{cm^{-2}}$, (d) 1.43 W $\mathrm{cm^{-2}}$.

obtained from the intensity-dependent experiments are indicated as the closed-circle symbol in Fig. 8. It was confirmed that the rate of reduction became faster as the ultrasonic intensity increased. It seems that the size of the gold particles is little affected by the strength of the shock waves because the smaller particles were formed at the stronger ultrasound intensity. The behavior of the gold particles under sonication is also discussed in a later section.

The relation between the size of the formed gold particles and the rate of gold(III) reduction was analyzed on the basis of the material balance. Assuming the formation of monodispersed gold nanoparticles with a spherical shape, the material balance is shown as Eq. 11:

$$(4/3)\,\pi\,(D/2)^3\rho\,N = CM \tag{11}$$

where D, ρ, N, C and M are the diameter of the formed particle (m), the density (kg $\mathrm{m^{-3}}$), the number of particles ($\mathrm{m^{-3}}$), the initial concentration of the metal ions (mol $\mathrm{m^{-3}}$) and the molecular weight (kg $\mathrm{mol^{-1}}$), respectively. Thus, D can be expressed as follows:

$$D = (6CM/\pi\rho N)^{1/3} \tag{12}$$

The total number of formed gold particles (N) should be correlated to the number of formed nuclei. In addition, the nuclei number should also correspond to the initial rate of gold(III) reduction ($\mathrm{d}C/\mathrm{d}t$). Thus, the following equation could be assumed:

$$N \propto (\mathrm{d}C/\mathrm{d}t) \tag{13}$$

Therefore, Eq. 12 could be roughly expressed as follows:

$$D \propto (6CM/\pi\rho)^{1/3}\cdot(\mathrm{d}C/\mathrm{d}t)^{-1/3} \tag{14}$$

Equation 14 can adequately account for the present experimental results such that the size of the formed gold particles decreases with the increasing rate of gold(III) reduction. The broken line in Fig. 8 is drawn as a visual aid.

On the other hand, if strong shock waves were generated, it would be expected that the size of the gold particles should become larger at the higher intensities so that a clear relationship between the rate of reduction and the particle size could not be obtained as seen in Fig. 8. The observed clear relation between them indicates that shock waves generated in the present irradiation system might be extremely weak. Consequently, our experimental results imply that the initial rate of gold(III) reduction strongly affects the nucleation process of the gold particles: The size of the gold particles depends on the number of the gold nuclei which correspond to the rate of reduction.

The cavitation bubbles with an extremely high temperature and high pressure were locally generated by the ultrasonic irradiation in solution. Their size and lifetime were calculated to be about several micrometers and less than sub-microseconds, respectively, in the 200 kHz irradiation system.[27] Thus, the radical reactions that proceeded in the bulk solution could be regarded as a mild condition at around room temperature. Analogous to this, the nucleation and growth of the gold particles is also suggested to occur in the bulk solution at such mild temperatures.

Ultrasound is generally used to disperse or agglomerate some particles or powders in solution by use of its mechanical effects, such as micro-jet impacts and shock waves, but the behavior of colloidal nanoparticles under sonication has not yet been clarified. It has been reported that the transition metal particles in the microns range are subjected to shock waves induced by the irradiation of a 20 kHz ultrasonic generator, resulting in the occurrence of interparticle collisions via a melting process.[28] On the other hand, the application of high-frequency ultrasound is suitable for cleaning a silicone wafer without any damage.[29] It appears that the mechanical effects due to the cavitation are attributed to the size of the collapsing bubbles: When the sizes of the collapsing bubbles are larger, the stronger mechanical effects would emerge. Therefore, mechanical effects would be relatively weak in the present 200 kHz sonication system in comparison with a conventional low-frequency sonication system.[30] In practice, various types of nanoparticles could be successfully formed without any aggregation by ultrasonic irradiation in the presence of stabilizers.[8,9,31] If any mechanical effects affected the growth of the particles, the size of the gold particles should not consistently increase with the decreasing rate of gold(III) reduction for the different experimental parameters. Accordingly, if the sonochemical nucleation and/or growth process of metal clusters and nanoparticles was hardly affected by the ultrasounds, the present results might also be applied to the interpretations of the formation process in a conventional reduction system.

Conclusion

In the present study, the sonochemical formation of gold particles was carried out in the presence of a small amount of 1-propanol to minimize the effects of organic molecules on the nucleation or growth processes of the gold particles. The rates of sonochemical reduction and the size of the formed particles could be changed by selecting the irradiation parameters, in spite of using the same starting materials and the same initial concentrations. The rate of gold(III) reduction strongly affected the sizes of the formed gold nanoparticles. When a high frequency was used, physical effects due to the cavitation on the nucleation in the nano-scale might be quite small. In addition, the effects of the ultrasonic cavitation on colloidal dispersion systems would be somewhat different in the size of the colloidal particles between the nano- and micro-meter ranges.

In the near future, by selecting stabilizers and combining organic accelerators as well as by applying the irradiation parameters clarified in the present study, transition metal nanoparticles having various particle sizes and distributions could be formed.

References

1 a) L. G. Olson, Y. S. Lo, T. P. Jr. Beebe, and J. M. Harris, *Anal. Chem.*, **73**, 4268 (2001). b) B. Neiman, E. Grushka, and O. Lev, *Anal. Chem.*, **73**, 5220 (2001).

2 a) A. Kusumi, Y. Sako, and M. Yamamoto, *Biophys. J.*, **65**, 2021 (1993). b) J. W. Slot, and H. J. Geuze, *J. Cell. Biol.*, **90**, 533 (1981).

3 P. Mulvaney, *MRS Bull.*, **26**, 1009 (2001).

4 a) M. Haruta, and M. Date, *Appl. Catal., A*, **222**, 427 (2001). b) M. Valden, X. Lai, and D. W. Goodman, *Science*, **281**, 1647 (1998).

5 a) F. Meriaudeau, T. Downey, A. Wig, A. Passian, M. Buncick, and T. L. Ferrell, *Sens. Actuators, B*, **54**, 106 (1999). b) Y. Jin, X. Kang, Y. Song, B. Zhang, G. Chng, and S. Dong, *Anal. Chem.*, **73**, 2843 (2001).

6 I. Tanahashi, Y. Manabe, T. Tohda, S. Sasaki, and A. Nakamura, *J. Appl. Phys.*, **79**, 1244 (1996).

7 a) M. A. EL-Sayed, *Acc. Chem. Res.*, **34**, 257 (2001). b) N. R. Jana, L. Gearheart, and C. J. Murphy, *Langmuir*, **17**, 6782 (2001). c) R. M. Crooks, M. Zhao, L. Sun, V. Chechik, and L. K. Yeung, *Acc. Chem. Res.*, **34**, 181 (2001). d) D. V. Leff, P. C. Ohara, J. R. Heath, and W. M. Gelbart, *J. Phys. Chem.*, **99**, 7036 (1995). e) C. H. Walker, J. V. St. John, and P. Wisian-Neilson, *J. Am. Chem. Soc.*, **123**, 3846 (2001). f) B. V. Enustun, and J. Turkevich, *J. Am Chem. Soc.*, **85**, 3317 (1963). g) H. Hirai, Y. Nakao, and N. Toshima, *Chem. Lett.*, **1978**, 545. h) G. Schmid, R. Pugin, T. Sawitowski, U. Simon, and B. Marler, *Chem. Commun.*, **1999**, 1303. i) T. Yonezawa, S. Onoue, and N. Kimizuka, *Langmuir*, **17**, 2291 (2001). j) K. Esumi, A. Suzuki, A. Yamahira, and K. Torigoe, *Langmuir*, **16**, 2604 (2000). k) S. Chen, and K.

Kimura, *Langmuir*, **15**, 1075 (1999). l) J. H. Hodak, A. Henglein, and G. V. Hartland, *J. Phys. Chem. B*, **104**, 9954 (2000). m) M. Y. Han, and C. H. Quek, *Langmuir*, **16**, 362 (2000).

8 Y. Nagata, Y. Mizukoshi, K. Okitsu, and Y. Maeda, *Radiat. Res.*, **146**, 333 (1996).

9 a) K. Okitsu, H. Bandow, Y. Maeda, and Y. Nagata, *Chem. Mater.*, **8**, 315 (1996). b) K. Okitsu, Y. Mizukoshi, H. Bandow, Y. Maeda, T. Yamamoto, and Y. Nagata, *Ultrason. Sonochem.*, **3**, 249 (1996).

10 F. Grieser, R. Hobson, J. Sostaric, and P. Mulvaney, *Ultrasonics*, **34**, 547 (1996).

11 a) A. Gedanken, R. Reisfeld, E. Sominski, O. Palchik, Y. Koltypin, G. Panczer, M. Gaft, and H. Minti, *J. Phys. Chem. B*, **104**, 7057 (2000). b) G. Dantsin, and K. S. Suslick, *J. Am. Chem. Soc.*, **122**, 5214 (2000). c) N. A. Dhas, A. Ekhtiarzadeh, and K. S. Suslick, *J. Am. Chem. Soc.*, **123**, 8310 (2001). d) W. Chen, W. Cai, Z. Zhang, and L. Zhang, *Chem. Lett.*, **2001**, 152.

12 K. Okitsu, A. Yue, S. Tanabe, H. Matsumoto, and Y. Yobiko, *Langmuir*, **17**, 7717 (2001).

13 T. Kimura, T. Sakamoto, J-M. Leveque, H. Sohmiya, M. Fujita, S. Ikeda, and T. Ando, *Ultrason. Sonochem.*, **3**, 157 (1996).

14 Y. Mizukoshi, K. Okitsu, H. Bandow, Y. Nagata, and Y. Maeda, *Bunseki Kagaku*, **45**, 327 (1996).

15 Y. T. Didenko, W. B. McNamara, and K. S. Suslick, *J. Am. Chem. Soc.*, **121**, 5817 (1999).

16 Y. Nagata, H. Okuno, Y. Mizukoshi, and Y. Maeda, *Chem. Lett.*, **2001**, 142.

17 A. S. Ghosh-Mazumadar, and E. J. Hart, *Adv. Chem. Ser.*, **81**, 231 (1968).

18 V. Misik, and P. Riesz, *Ultrason. Sonochem.*, **3**, 173 (1996).

19 K. Kurihara, J. Kizling, P Stenius, and J. H. Fendler, *J. Am. Chem. Soc.*, **105**, 2574 (1983).

20 E. A. Neppiras, *Phys. Rep.*, **61**, 159 (1980).

21 a) C. Krishna, T. Kondo, and P. Riesz, *J. Chem. Phys.*, **93**, 5166 (1989). b) Y. T. Didenko, and S. P. Pugach, *Ultrason. Sonochem.*, **1**, 9 (1994). c) F. R. Young, *J. Acoust. Soc. Am.*, **60**, 100 (1976). d) W. B. McNamara Ⅲ, Y. T. Didenko, and K. S. Suslick, *Nature*, **401**, 772 (1999).

22 "Kagaku Binran," Maruzen, Japan (1984), Vol. Ⅱ, p. 71.

23 "Kagaku Binran," Maruzen, Japan (1984), Vol. Ⅱ, p. 159.

24 A. Henglein, *Ultrasonics*, **25**, 6 (1987).

25 J. Buttner, M. Gutierrez, and A. Henglein, *J. Phys. Chem.*, **95**, 1528 (1991).

26 Y. Mizukoshi, H. Nakamura, H. Bandow, Y. Maeda, and Y. Nagata, *Ultrason. Sonochem.*, **6**, 203 (1999).

27 The resonance radius (R_0) of the bubbles and the collapsing time (τ) was calculated to be ca. 13 μm and ca. 0.67 μs, respectively, on the basis of Neppiras' equations [Ref. 20] with the parameters of 1.256×10^5 sec^{-1} for ω_a and 1000 kg/m^3 for ρ, and the assumed parameters of 1.01325×10^5 N m^{-2} for P_h and 2.0265×10^5 N m^{-2} for P_a. In addition, the radius of the hot bubbles could be calculated to be ca. 4 μm according to the equation of adiabatic compression, in which the temperature of the resonance bubbles and the hot bubbles, and γ value were 293 K, 3500 K and 1.67, respectively.

28 S. J. Doktycz, and K. S. Suslick, *Science*, **247**, 1067 (1990).

29 "Chou-onpa Binran," Maruzen, Japan (1999), pp. 669–677.

30 To discuss the cavitation strength related to mechanical effects (shock waves and microjet impacts, etc), the effects of cavitation on an immersed aluminum foil were investigated. The result showed that no pit attributed to cavitation damage was observed, suggesting that mechanical effects would be weak in the present 200 kHz irradiation system. On the other hand, a number of pits and holes on the foil were observed by irradiation using a conventional 28 kHz ultrasonic cleaner.

31 a) Y. Nagata, Y. Watanabe, S. Fujita, T. Dohmaru, and S. Taniguchi, *J. Chem. Soc., Chem. Commun.*, **1992**, 1620. b) Y. Mizukoshi, K. Okitsu, T. Yamamoto, R. Oshima, Y. Nagata, and Y. Maeda, *J. Phys. Chem. B*, **101**, 5470 (1997). c) Y. Mizukoshi, R. Oshima, Y. Maeda, and Y. Nagata, *Langmuir*, **15**, 2733 (1999). d) K. Okitsu, A. Yue, S. Tanabe, and H. Matsumoto, *Chem. Mater.*, **12**, 3006 (2000). e) K. Okitsu, M. Murakami, S. Tanabe, and H. Matsumoto, *Chem. Lett.*, **2000**, 1336. f) Y. Mizukoshi, T. Fujimoto, Y. Nagata, R. Oshima, and Y. Maeda, *J. Phys. Chem. B*, **104**, 6028 (2000). g) Y. Mizukoshi, E. Takagi, H. Okuno, R. Oshima, Y. Maeda, and Y. Nagata, *Ultrason. Sonochem.*, **8**, 1 (2001). h) K. Okitsu, A. Yue, S. Tanabe, and H. Matsumoto, *Bull. Chem. Soc. Jpn.*, **75**, 449 (2002).